Effect of PAN-based and pitch-based carbon fibres on microstructure and properties of continuous Cf/ZrB2-SiC UHTCMCs

Effect of PAN-based and Pitch-based carbon fibres on microstructure and properties of continuous C_f/ZrB_2-SiC UHTCMCs

D. Sciti[1], L. Zoli[1], A. Vinci[1], L. Silvestroni, S. Mungiguerra[2], P. Galizia[1],

[1] *National Research Council, Institute of Science and Technology for Ceramics, Via Granarolo 64, 48018 Faenza, Italy*

[2]*University "Federico II", Department of Industrial Engineering, Aerospace Division, P.le Tecchio 80, 80125 Napoli, Italy*

ABSTRACT

In this paper the microstructure and mechanical properties of two different C_f/ZrB_2-SiC composites reinforced with continuous PyC coated PAN-derived fibres or uncoated pitch-derived fibres were compared.

Pitch-derived carbon fibres showed a lower degree of reaction with the matrix phase during sintering compared to PyC/PAN-derived fibres. The reason lies in the different microstructure of the carbon. The presence of a coating for PAN-derived fibres was found to be essential to limit the reaction at the fibre/matrix interface during SPS. However, coated bundles were more difficult to infiltrate, resulting in a less homogeneous microstructure.

As far as the mechanical properties are concerned, specimens reinforced with coated PAN-derived fibres provided higher strengths and damage tolerance than uncoated pitch-derived fibres, due to the higher degree of fibre pull-out. On the other hand, the weaker fibre/matrix interface resulted in lower interlaminar shear, off-axis strength and ablation resistance.

Keywords
UHTCMC, Carbon fibres, mechanical properties, microstructure, self-healing.

1. Introduction

Ultra-high temperature ceramic matrix composites (UHTCMCs) are a novel class of materials obtained from the combination of ultra-high temperature ceramics (UHTCs) and carbon or silicon carbide fibres/preforms [1]. The added value of these composites is the possibility to couple the damage tolerance of fibre reinforced composites with the refractoriness of UHTCs. [2,3]

The target is the achievement of a futuristic generation of reusable materials for application above 2000°C in aerospace, military and nuclear applications [4–10]. This niche of materials has recently become a new field of research and the latest review papers by Rueschoffs et al. [11] and

Binner et al. [12] have reported a large escalation of publications in the last two years. At the moment the research is still very focused on the design and processing of these composites.

The UHTCMC class includes materials with both short and continuous fibres and most of the research is concerned with the use of carbon fibres [12]. The fibres confer damage tolerance and thermal shock resistance to the UHTC matrix, the UHTC phase protects the fibres during elevated temperature oxidation, ensuring good ablation and erosion behaviour even without a post processing environmental external coating. Similar to other CMC composites, the matrix/fibre interface plays a fundamental role and should be weak enough to have sufficient fibre pullout at fracture and dense enough to hinder penetration of corrosive/oxidative gases during exposition.

Several processing techniques have been adopted for the fabrication of UHTCMCs, most of which are readapted from the CMC science. The most important and studied methods are:

- polymer infiltration and pyrolysis (PIP), where the UHTC phase is added to a SiC precursor [13]. This method allows the manufacturing of large pieces with complex preforms, but the lack of UHTC precursors results in a relatively low content of UHTC phase in the final products.
- reactive melt infiltration (RMI), where the carbon preforms are infiltrated with Zr-containing melts [14]. This technique has the advantage to be very fast and versatile, but the Zr-based melt easily reacts and degrade the carbon fibres.
- chemical vapour infiltration (CVI) with gaseous precursors of carbide phases, or with C precursors preceded by an infiltration stage with a UHTC containing slurry [15,16]. This is by far the best processing route for achieving large pieces, stress-free composites with a desired weak fibre matrix interface. Conventional CVI is considered an expensive and time consuming technique, therefore researchers at the University of Birmingham have recently developed a very appealing variant, called radio frequency heated chemical vapour infiltration (RF-CVI), where the inverse temperature profile generated by RF heating allows to get very high values of matrix density in hours rather than weeks. [16]

Authors of the present work have focused their effort on manufacturing of UHTCMCs via slurry infiltration and densification by hot pressing, reporting promising results in previous papers. [17,18] Recently, the feasibility of the SPS process for the consolidation of UHTCMCs [19] has been also demonstrated, revealing that this class of composites can be densified in a few minutes. Overall, this process is in its infancy and all its multiple facets still have to be deeply investigated. Current limitations include the difficulty to use 2.5D or 3D preforms, because the fibres disposed along the direction of the applied mechanical load can be damaged during the thermal treatment.

Another important issue is the choice of the carbon fibre type. Polyacrylonitrile (PAN)-based fibres are the preferred option in the fabrication of C/C composites, thanks to the high tenacity and

strength. However, during densification at elevated temperature in a ZrB_2-based matrix they were strongly damaged. [19] Alternative commercial products are the so-called pitch-based fibres, that are derived from a polycyclic aromatic mesophase pitch. These fibres were found to be more suitable for the manufacturing of UHTCMCs, thanks to the lower reactivity with the boride phase [19].

Beside all the possible techniques to manufacture UHTCMCs, there is still a lot of variability in the design of these materials. Consequently, comparison of mechanical properties amongst published data is very difficult and the models that describe the relationships between experimental values and features like matrix composition, fibre content/type/architecture and their combinations are still missing or not fully developed for this niche of composites.

In this work we illustrated two notional models of UHTCMCs obtained by slurry impregnation and spark plasma sintering, with the same matrix, but different types of carbon fibres, e.g. pitch-based and PyC-coated PAN-based. The scope was to highlight the differences in processing, microstructure and final performance on small scale samples.

2. Experimental

Commercial products were used for the production of UHTCMCs: ZrB_2 (Grade B, H.C. Starck, Germany, particle size range 0.5-6 µm, impurities (wt%): 0.2 C, 1.3 O, 0.19 N, 0.1 Fe, 1.4 Hf); α-SiC (Grade UF-25, H.C. Starck, Germany, D50 0.45 µm); unidirectional (UD) preforms of pitch-based C_f (XN80-6K, Granoc, Japan), diameter 10 µm, uncoated. PAN-derived carbon fibres (T800HB-6000, TORAYCA, Japan), diameter 5 µm, were coated with a pyrolytic carbon (PyC) coating, average thickness ~ 0.4 µm) through a proprietary process of AIRBUS (Airbus Defence and Space GmbH, 82024 Taufkirchen, Germany).

Water-based slurries containing a 90 vol% ZrB_2 - 10 vol% SiC powder mixture were prepared according to previously published procedure [18] and used to impregnate the pitch-based preforms. For the PyC-coated PAN-based carbon fibres, a filament winding equipment available at AIRBUS-DS was used to produce unidirectional fibre sheets impregnated with the slurry. Then, impregnated layers of both types of preforms were overlapped in 0/0° stacking sequence to get unidirectional composites (UD samples).

Discs with diameter Ø = 40 mm were then sintered by spark plasma sintering [19] (SPS furnaces HPD25, FCT Systeme GMBH, Germany) under vacuum at 1850°C, with 200 s holding time, 100 °C/min heating rate and 40 MPa applied pressure. The temperature was recorded through a pyrometer placed at the top of the machine and pointing at the centre of the blank (5 mm over the top surface). The bulk density of the sintered pellets was measured using the Archimedes' method.

The microstructures were analysed on polished and fractured surfaces using field emission scanning electron microscopy (FE-SEM, Carl Zeiss Sigma NTS Gmbh Öberkochen, Germany). The fibre volumetric content and the residual porosity were measured by image analysis (Image-Pro Analyzer 7.0, v.7, Media Cybernetics, USA) on SEM micrographs of polished sections, to determine the final compositions.

Four-point bending tests were performed on 25.0 × 2.5 × 2.0 mm^3 bars (length by width by thickness, respectively) at RT (σ) in both longitudinal and transversal directions and at 1500 °C in Ar atmosphere ($\sigma_{1500°C}$) in the longitudinal direction. Chevron notched beams (CNB) specimens of 25.0 × 2.0 × 2.5 mm^3 (length by width by thickness, respectively) were used for toughness tests (K_{Ic}). The test bars were notched with a 0.1 mm-thick diamond saw; the chevron-notch tip depth and average side length were about 0.12 and 0.80 of the bar thickness, respectively. All the bars were fractured using a semi-articulated four-point fixture with a lower span of 20 mm and an upper span of 10 mm, using a Zwick-Roell Z050 screw-driven load frame. The crosshead speed was 1 mm/min and 0.05 mm/min for σ and K_{Ic}, respectively. The Work-of-Fracture (WoF) was calculated from the CNB test as the area below the load-displacement curve divided by the double of the projected real surface. With the same machine, three-point bending tests were performed on 25.0 × 5.0 × 3.0 mm^3 bars (length by width by thickness, respectively) in order to evaluate the interlaminar shear strength (ILSS) by the short beam shear (SBS) test method. A span of 15 mm and a crosshead speed 1 mm/min were used. For each test, at least three bars were used.

The oxidation resistance to dissociated plasma of oxygen and nitrogen was tested through the arc-jet wind tunnel SPES available at the University of Naples "Federico II". Small sized UHTCMC models were machined from both samples and exposed to a supersonic high enthalpy gas mixture of nitrogen (0.8 g/s) and oxygen (0.2 g/s) (nominal Mach number 3). During the test, the arc power of the plasma torch was gradually increased, leading to an increase of pressure and temperature and enthalpy, reaching a maximum value of 20 MJ/kg for 120 s. Further experimental set-up details are reported in dedicated works. [20,21] Post-test analyses of the exposed surfaces were carried out using scanning electron microscopy. For the sake of comparison, composites were hereinafter labelled as PAN or PITCH, depending on the type of reinforcement used.

3. Results and discussion

3.1 Microstructural features

Physical properties of PAN and PITCH composites are summarized in Table 1. Apparently, experimental density, residual porosity and fibre volumetric content were quite different in the two

composites, as explained later. In the case of fibre volumetric content, it can be noticed that we indicated ranges in Table 1. Indeed, uncertainty in the exact quantification of fibre volumetric content was due to both intrinsic limitation of the method (image analysis) and to possible local variations in the microstructure.

Microstructural features of the starting fibres and composites are shown in Fig. 1a-f. PyC-coated PAN-based carbon fibres (supplied by AIRBUS DS) $\phi \sim 5$ µm, have a turbostratic structure and are quite reactive in the sintering environment with a UHTC matrix. The 400 nm thick protective coating is visible in Fig. 1a. Fig. 1b-c shows microstructure and interface in the final PAN composite. When PyC-coated PAN-based carbon fibres were used, the matrix phase distribution was partially uneven, Fig. 1b, because the coating procedure caused the fibres to stick together and the liquid slurry could not penetrate the bundles. As a consequence, the amount of slurry absorbed was lower, explaining the higher fibre volumetric content with respect to the PITCH composite, 45 vs 55%. For the same reason, e.g. the lower amount of matrix phase, the densification was somewhat inhibited, therefore the final porosity of this composite was higher, around 18%. Since infiltrated space amongst the fibres can be as long as the fibre length, we deduced that a part of this porosity was open. The resulting density was as low as 2.8 g/cm^3 (see Table 1). As for the matrix-fibre interface, the presence of the coating was effective in limiting the carbon reactivity with the matrix phases, since it acted as a buffer layer. Spurious phases such as SiC and ZrC were also detected (see Fig. 1c). ZrC formation was the result of carbo-thermal reduction of ZrO_2 present as surface oxide onto ZrB_2 grains at the carbon/matrix interface, as previously reported. [17] As expected, the presence of both fibre coating and residual porosity favoured a high degree of fibre pull-out, due to weak interfaces, see Fig. 2e. On the other hand, pitch-based fibres, $\phi \sim 10$ µm, are characterized by a higher degree of graphitization and a typical onion structure Fig. 1d. This structure allowed their use in a severe sintering environment at high temperature and under high pressure even without a protective coating [1,22]. The typical microstructure overview and fibre/interface features of this composite are reported in Figs. 1 e, f. The PITCH composite had a higher density, 3.6 g/cm^3, porosity around 7% and fibre volumetric content in the range 40-45 vol%. In this case, the limited amount of residual porosity and the homogeneous dispersion of the matrix phase in the preforms suggested that pores were mostly closed. The fibre/matrix interface was quite smooth and the fibre pull-out (see Fig. 2f) was much more limited compared to the previous case [1,22].

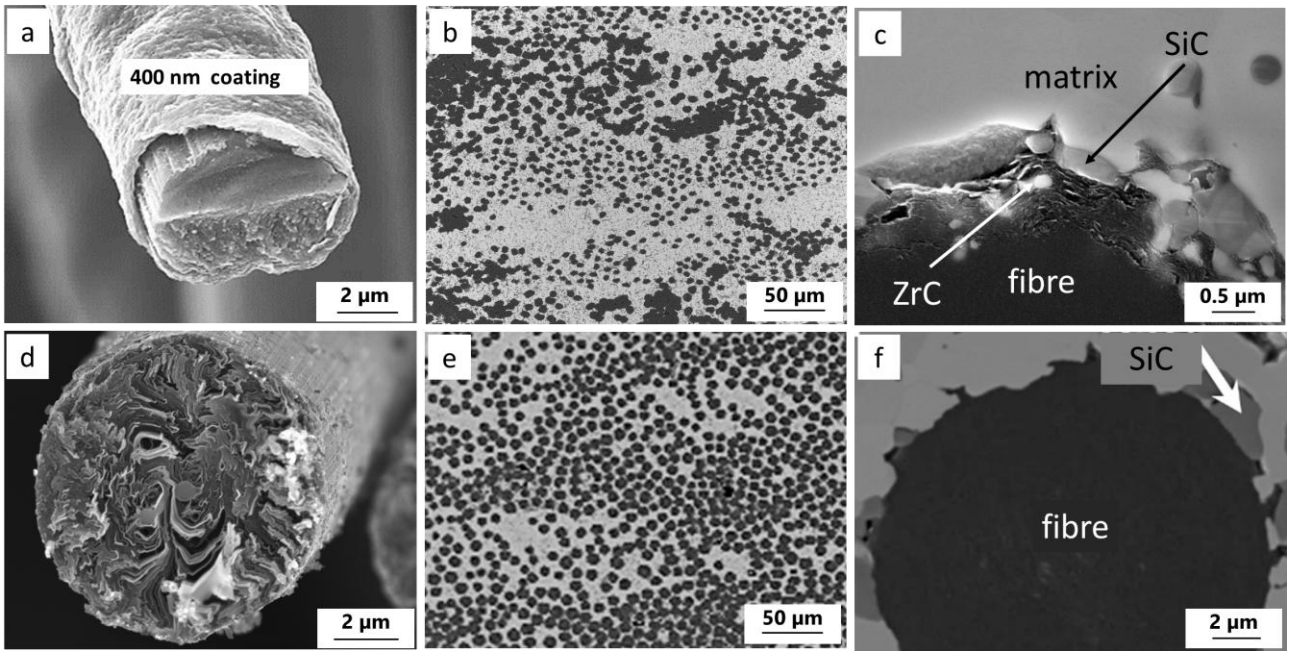

Fig.1. Fibre features and microstructural features of the composites. a) A raw PyC-coated PAN-based carbon fibre, b) polished microstructure of the PAN sample and (c) PAN fibre/matrix interface, with SiC and ZrC phases d) A raw Pitch-based carbon fibre, e) polished microstructure and f) strong fibre/matrix interface of the PITCH sample.

3.2 Mechanical properties and ablation resistance

Mechanical properties are summarized in Table 1, for PAN and PITCH samples.

Table 1: Properties of PAN-based and Pitch-based fibre reinforced composites

Property	**PAN**	**PITCH**
Density, ρ (g/cm^3)	2.8±0.1	3.6±0.1
Porosity, P (%)	~18	~7
Fibre volumetric content, FVC (%)	50-55	40-45
Longitudinal flexural strength, σ_1 (MPa)	300±50[a]	260±20[b]
Transverse flexural strength, σ_2 (MPa)	25±1	61±13
Interlaminar shear strength by SBS, τ (MPa)	21±2	37±5[b]
Longitudinal flexural strength at 1500 °C, $\sigma_{1500°C}$ (MPa)	370±110[a]	440±30[b]
Fracture toughness by CNB, K_{Ic} (MPa·m$^{0.5}$)	14.6±3.0	8.7±0.4
Work-of-Fracture by CNB, WoF (kJ/m^2)	4.6±1.2	0.5±0.1

[a] Conservative value owing to shear mode failure.
[b] Conservative value owing to tensile and shear mixed mode failure.

The room temperature flexural strength was higher for PAN composite owing to the higher strength of the constituent fibres and their higher content. From the load-displacement curves (Fig.

2a), it can be seen that both samples suffered from interlaminar shear. Hence, the reported flexural strengths can be considered conservative values, due to unfavourable span-to-thickness ratio. Indeed, flexural tests on larger specimens are expected to reveal an increase of the ultimate flexural stress by limiting the interlaminar shear stresses during bending moment, especially for PAN specimens that exhibited a low ILSS.

Concerning the transverse strength of 0/0° composites, the fibres could not effectively bear the load transferred from the matrix in this direction, and they predominantly acted as defects. Thus, the transverse strength was quite dependent on the fibre-matrix bonding strength and the matrix strength. For the PAN composite, due to lose matrix and weak interfacial bonding strength, the flexural strength was 3 times lower for PAN compared to PITCH composites. The load displacement curves however showed that in this direction the sample displayed a brittle behaviour (Fig. 2b), i.e. after reaching the maximum load, a catastrophic failure occurred. Strengths in the order of 60-70 MPa were obtained with a similar composite characterized by the same type of fibre, FVC, and matrix porosity although reactive sintering was involved [23]. Investigation about strength retention in this direction showed that these composites are insensitive to flaws of about 50 μm despite the brittle behaviour dominated by the matrix - in other words, flaws of at least 50 μm are already present in these composites characterized by densified matrix [23]. Analogously to the transverse strength, PAN sample was also more prone to interlaminar fracture (Fig.2 c), with interlaminar shear strength (ILSS) of 20 MPa, i.e. more than halved as compared to PITCH. On the other hand, PITCH samples did not show a interlaminar shear dominated failure and for this reason we can only state that ILSS should be higher than 40 MPa, which is the maximum interlaminar shear stress withstood during the test. Again, the lower degree of penetration of the slurry in the fibre bundles made the PAN composite more prone to delamination compared to PITCH.

The 1500°C flexural strength confirmed the general tendency of these composites, e.g. the improvement of mechanical properties with increasing temperature. For PAN sample, longitudinal strength passed from 300 to 370 MPa, for PITCH the increase was even more marked, from 255 to 440 MPa. This improvement was related to both increase of mechanical properties of Carbon fibres with temperature [24] and release of thermal residual stresses developed during the sintering process. [25] This is in agreement with recent papers [1, 25–28], where release of thermally-induced tensile stresses in matrix was considered responsible of strength increase at elevated temperature.

Measure of the fracture toughness for this kind of composites can be debateable. Commonly, the SENB technique is used, however the theoretical condition of having a sharp notch is quite hard to be satisfied with this technique. On the other hand, using the CNB technique, the

accuracy of the chevron initial crack is much higher, but the obtained values could be slightly overestimated due to R-curve behaviour of these composites, not yet studied for this class of composites. Nevertheless, using the same technique for such different composites could at least give a term of comparison of the values. In the case of PAN sample, the average value was 14.6 MPa $m^{0.5}$, and the work of fracture (WoF) was around 4.6 kJ/m^2 (Fig. 2e). This value was much higher than those reported in the literature, generally lower than 2 kJ/m^2 [29]. For PITCH sample, the fracture toughness recorded was 8.7 MPa $m^{0.5}$, with a WoF of 0.5 kJ/m^2. Indeed, the characteristics of the interface, which allowed a higher pull-out in case of PAN-based fibres (Fig. 2e,f), as well as the higher content of fibres were factors explaining the higher values recorded for PAN sample. Similar results about the effect of pyrolytic carbon coating were obtained by Zhang et al. [29]. They also observed that the coating promoted the fibre pull-out and led to a non-brittle fracture mode. However, owing to the more uneven fibre distribution in PAN sample, all the reported mechanical responses resulted more scattered with respect to the PITCH sample (Fig. 2d). The dispersion of values may be narrower if larger specimens are fractured, as already mentioned for flexural strength.

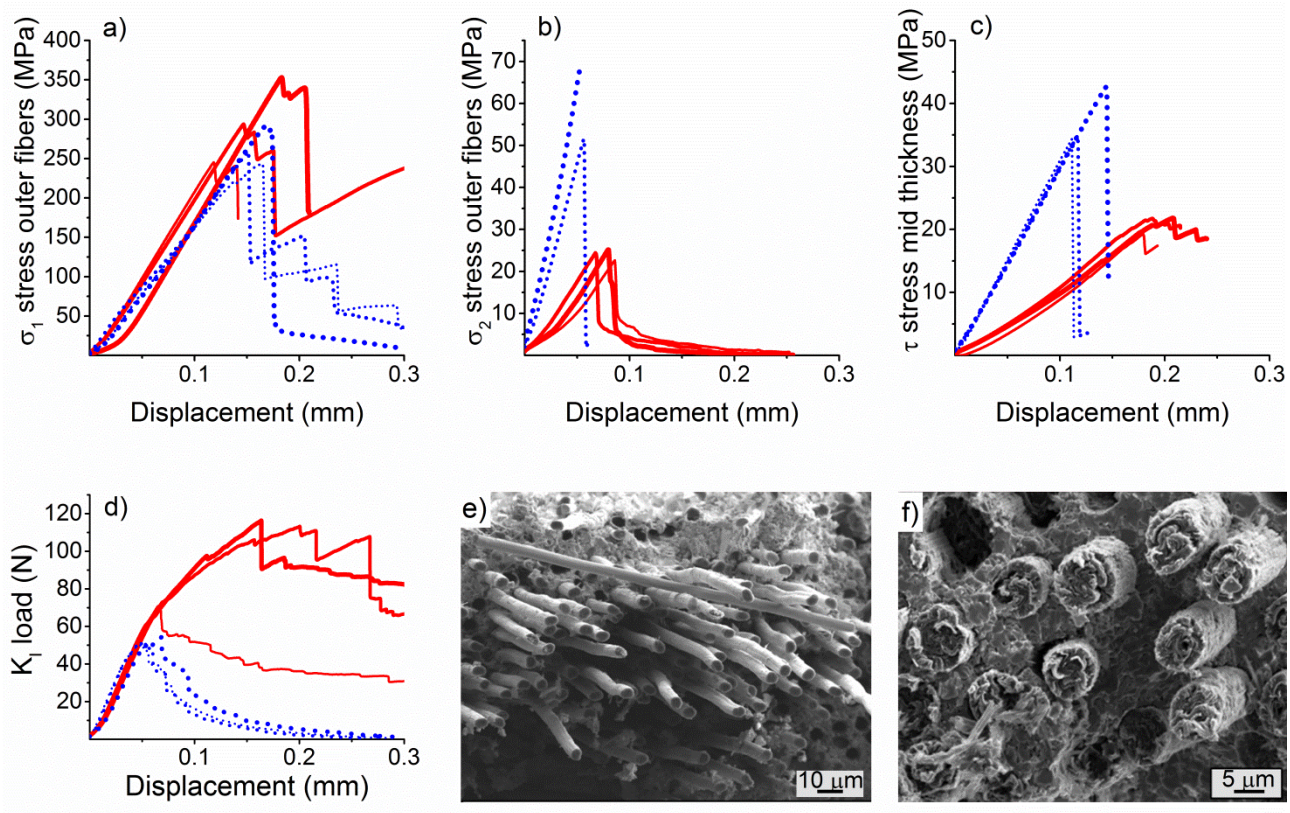

Fig. 2. Stress-displacement curves of PAN (solid curves) and PITCH (dotted curves) specimens for a) longitudinal and b) transverse bending strength, and c) interlaminar shear strength. d) Fracture toughness load-displacement curves and related fracture surfaces SEM images of e) PAN and f) PITCH

Arc-jet tests of PAN and PITCH-based composites were extensively discussed in previous papers [20,21]. All the samples tested underwent a rapid increase of the surface temperature, exceeding 2400 K and attaining in some cases almost 2800 K, associated to the so-called "jump of radiance" generally observed for UHTC-based materials. [30] Visually, both sample surfaces changed their colour from the original dark grey to white, due to the oxidation of ZrB_2 to ZrO_2 and vaporization of grey surface silica. Although a detailed analysis of the composites microstructure is out of the scope of the present work, some considerations can be done. For PITCH sample, the weight loss was estimated as the difference between final and initial weight, normalized to the period of time during which the sample temperature was >1000 °C, e.g. 450 s. The net weight loss was almost negligible, $2 \cdot 10^{-4}$ g/s, and was accompanied by a slight volume expansion. On the contrary, for PAN-reinforced composites, a proper evaluation of weight and volume variations was not possible due to oxide spalling. Weight variations were due to concurrent phenomena, e.g. increase of weight due to oxidation of ZrB_2 and SiC to the corresponding oxides, whilst decrease of weight was caused by Cf vaporization on the surface and/or eventual detachment of the oxidized layer from the unoxidised bulk. In the case of the PAN sample the oxide layer showed the tendency to spall-off from the bulk due to CTE mismatch with the unreacted bulk and brittleness of the oxide scale, see Figs. 3 a,b. For this composite, the higher amount of fibres, 50-55 vs 40-45 vol%, the formation of stuck fibres in the matrix during the coating deposition, and the presence of higher residual porosity, ~18 vs~ 7 vol%, made it difficult for the matrix to exert its protective action. On the contrary, PITCH samples demonstrated a promising self-healing ability, testified by the capability of rapid closure of pores generated by fibre burning and good adhesion of the scale to the bulk, see Figs. 3 d,e.

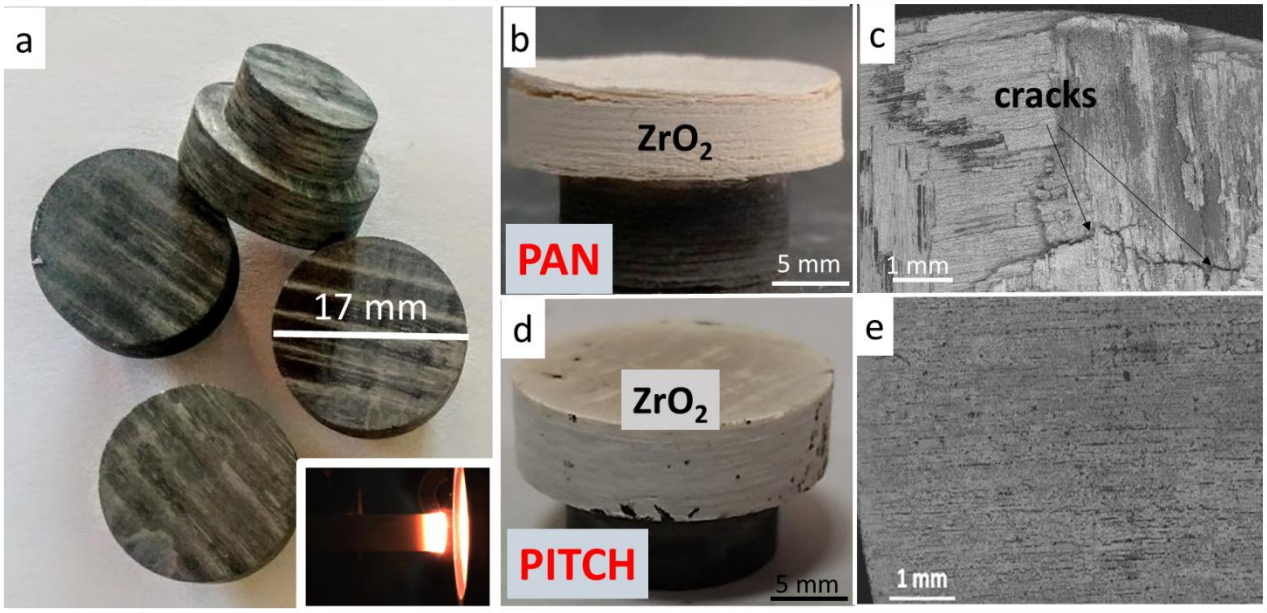

Fig.3. a) As machined arc-jet prototypes with an inset of the test recorded by thermo-camera, b) visual appearance of PAN sample after the test showing ZrO_2 spalling, c) surface microstructure detected by SEM showing oxide discontinuities and cracks. d) Visual appearance of PITCH sample after the test, e) surface microstructure by SEM.

The micrographs reported in Fig. 3c and Fig. 3e, confirmed the optical view, the surface oxide layer was compact in PITCH composite but cracked and discontinuous in PAN composite because borosilicate glass was not able to repair the large defects and voids left by fibre vaporization.

In summary, this study highlighted that the choice of the fibre strongly affects the microstructure and final performance of UHTCMCs. First of all, the different characteristics of PyC-coated PAN and uncoated pitch-based carbon fibre preforms affected the composite preparation, resulting in different levels of matrix homogenization, porosity and diverse fibre concentration.

Similar to conventional CMCs, flexural strength and fracture toughness were positively affected by higher fibre strength, higher fibre volumetric fraction and the relatively weaker fibre/matrix interface, characteristics of the PAN composite. The use of PyC-coated PAN-based carbon fibres facilitated fibre pull-out and load transfer from the matrix to the fibre. On the contrary, transverse strength, interlaminar strength and oxidation resistance were mostly influenced by the compactness of the matrix and the stronger matrix-fibre interface, characteristics peculiar of UHTCMCs developed with pitch-derived fibres. Table 2 ultimately compares the performances of the two composites with respect to desired requirements.

Desired features of UHTCMCs	PAN	PITCH
Well integrated ultra-refractory matrix (UHTC) and C fibre fabric	Good	Excellent
Moderate density	Good	Average
Need of a fibre coating	High	Low
Low porosity to hinder penetration of corrosive/oxidative gases	Poor	Excellent
Fibre pull-out at fracture – weak interface	Excellent	Poor
Need of environmental protective coating	High	Low
Mechanical properties – Flexural strength, toughness	Excellent	Good
High temperature properties	Excellent	Excellent
Ablation resistance	Average	Excellent

Table 2: Comparison of UHTCMC features in relation to the desired requirements.

4. Conclusions

In this work we compared properties and microstructure of two UHTCMCs containing PyC-coated PAN-based or uncoated pitch-based carbon fibres. UHTCMCs were successfully fabricated by slurry infiltration and spark plasma sintering using different type of fibres, although the final fibre volumetric amount was different. This variability was due to the different characteristics of the fibre preforms and process and further work is necessary to fully control the fibre volumetric content during manufacturing. Highly homogenous fibre dispersion was achieved with pitch-based fibre fabrics, leading to low matrix porosity. The PyC coating was effective to protect PAN-based fibres during sintering at high temperature, facilitating pull-out and increasing the damage tolerance of the composite, but led to microstructure inhomogeneities owing to partial gluing of the fibre bundles during the coating application. Uncoated pitch-based fibres were well anchored to the UHTC matrix, resulting in a strong interface, with little pull-out.

Properties mostly determined by fibre strength and weak interface, such as strength and toughness, were higher when coated pan-based fibres were used as reinforcement. Properties primarily affected by matrix density and high interface strength, such as transverse strength, interlaminar shear strength and oxidation resistance, were higher for naked pitch-based composites, due to the most effective impregnation with the boride phase. The higher matrix porosity and fibre content of the PAN composite were indeed detrimental factors for the ablation resistance in arc-jet test.

This study showed that, at this stage of material development, a high number of requirements can be already satisfied when pitch-based C fibres are used for the manufacturing of UHTCMCs. Further improvement could be achieved with the design of a fibre coating suited for interfacing with the boride matrix, in order to have a weaker bond, but without hindering the slurry infiltration.

Overall, the results are promising for both types of composites and we believe there is still a high margin for improving their properties and performance. Further steps in the development of these materials process are the scale-up to manufacture test bars large enough for bending and tensile test and the full determination of thermo-mechanical properties and ablation behaviour.

Acknowledgements

The C^{3}HARME research project has received funding by the European Union's Horizon2020 research and innovation programme under the Grant Agreement 685594. Authors wish to acknowledge A. Schoberth (AIRBUS), P. Mittermeier (AIRBUS), F. Meistring (Arianegroup) for supplying coated PAN-based fibres and technical support in the filament winding procedure, C. Gutierrez, S. Rivera (Nanoker Research) for SPS cycles, R. Savino (University of Naples) for arc-jet tests.

Bibliography

[1] L. Zoli, A. Vinci, P. Galizia, C. Melandri, D. Sciti, On the thermal shock resistance and mechanical properties of novel unidirectional UHTCMCs for extreme environments, Sci. Rep. 8 (2018) 9148. doi:10.1038/s41598-018-27328-x.

[2] W.G. Fahrenholtz, G.E. Hilmas, I.G. Talmy, J.A. Zaykoski, Refractory diborides of zirconium and hafnium, J. Am. Ceram. Soc. 90 (2007) 1347–1364. doi:10.1111/j.1551-2916.2007.01583.x.

[3] E.P. Simonenko, N.P. Simonenko, V.G. Sevastyanov, N.T. Kuznetsov, ZrB_2/HfB_2–SiC Ceramics Modified by Refractory Carbides: An Overview, Russ. J. Inorg. Chem. 64 (2019) 1697–1725. doi:10.1134/S0036023619140079.

[4] N.P. Padture, Advanced structural ceramics in aerospace propulsion, Nat. Mater. 15 (2016) 804–809. doi:10.1038/nmat4687.

[5] D. Gosset, M. Dollé, D. Simeone, G. Baldinozzi, L. Thomé, Structural evolution of zirconium carbide under ion irradiation, J. Nucl. Mater. 373 (2008) 123–129. doi:10.1016/j.jnucmat.2007.05.034.

[6] C. Dickerson, Y. Yang, T.R. Allen, Defects and microstructural evolution of proton irradiated titanium carbide, J. Nucl. Mater. 424 (2012) 62–68. doi:10.1016/j.jnucmat.2012.02.005.

[7] M. Nakagawa, Y. Suzuki, A. Chiba, Y. Gotoh, R. Jimbou, M. Saidoh, Development of Boron Carbide-Carbon Fiber Composite Ceramics as Plasma Facing Materials in Nuclear Fusion Reactor (Part 1), J. Ceram. Soc. Japan. 105 (1997) 851–857. doi:10.2109/jcersj.105.851.

[8] L.M. Garrison, G.L. Kulcinski, G. Hilmas, W. Fahrenholtz, H.M. Meyer, The response of ZrB_2 to simulated plasma-facing material conditions of He irradiation at high temperature, J. Nucl. Mater. 507 (2018) 112–125. doi:10.1016/j.jnucmat.2018.04.016.

[9] A. Bhattacharya, C.M. Parish, T. Koyanagi, C.M. Petrie, D. King, G. Hilmas, W.G. Fahrenholtz, S.J. Zinkle, Y. Katoh, Nano-scale microstructure damage by neutron irradiations in a novel Boron-11 enriched TiB2 ultra-high temperature ceramic, Acta Mater.

165 (2019) 26–39. doi:10.1016/j.actamat.2018.11.030.
[10] A. Yehia, R. Vaßen, R. Duwe, D. Stöver, Ceramic SiC/B_4C/TiC/C composites as plasma facing components for fusion reactors, J. Nucl. Mater. 233–237 (1996) 1266–1270. doi:10.1016/S0022-3115(96)00155-9.
[11] L.M. Rueschhoff, C.M. Carney, Z.D. Apostolov, M.K. Cinibulk, Processing of fiber-reinforced ultra-high temperature ceramic composites: A review, Int. J. Ceram. Eng. Sci. (2020). doi:10.1002/ces2.10033.
[12] J. Binner, M. Porter, B. Baker, J. Zou, V. Venkatachalam, V.R. Diaz, A. D'Angio, P. Ramanujam, T. Zhang, T.S.R.C. Murthy, Selection, processing, properties and applications of ultra-high temperature ceramic matrix composites, UHTCMCs – a review, Int. Mater. Rev. (2019). doi:10.1080/09506608.2019.1652006.
[13] Q. Li, S. Dong, Z. Wang, G. Shi, Fabrication and properties of 3-D Cf/ZrB_2-ZrC-SiC composites via polymer infiltration and pyrolysis, Ceram. Int. 39 (2013) 5937–5941. doi:10.1016/j.ceramint.2012.11.074.
[14] M. Kütemeyer, T. Helmreich, S. Rosiwal, D. Koch, Influence of zirconium-based alloys on manufacturing and mechanical properties of ultra high temperature ceramic matrix composites, Adv. Appl. Ceram. 117 (2018) s62–s69. doi:10.1080/17436753.2018.1509810.
[15] L. Li, Y. Wang, L. Cheng, L. Zhang, Preparation and properties of 2D C/SiC–ZrB_2–TaC composites, Ceram. Int. 37 (2011) 891–896. doi:https://doi.org/10.1016/j.ceramint.2010.10.033.
[16] V. Rubio, P. Ramanujam, J. Binner, Ultra-high temperature ceramic composite, Adv. Appl. Ceram. (2018). doi:10.1080/17436753.2018.1475140.
[17] L. Zoli, A. Vinci, P. Galizia, C. Melandri, Di. Sciti, On the thermal shock resistance and mechanical properties of novel unidirectional UHTCMCs for extreme environments, Sci. Rep. (2018). doi:10.1038/s41598-018-27328-x.
[18] L. Zoli, D. Sciti, Efficacy of a ZrB_2–SiC matrix in protecting C fibres from oxidation in novel UHTCMC materials, Mater. Des. 113 (2017) 207–213. doi:10.1016/j.matdes.2016.09.104.
[19] L. Zoli, A. Vinci, P. Galizia, C.F. Gutièrrez-Gonzalez, S. Rivera, D. Sciti, Is spark plasma sintering suitable for the densification of continuous carbon fibre - UHTCMCs?, J. Eur. Ceram. Soc. (2019). doi:10.1016/j.jeurceramsoc.2019.12.004.
[20] S. Mungiguerra, G.D. Di Martino, A. Cecere, R. Savino, L. Silvestroni, A. Vinci, L. Zoli, D. Sciti, Arc-jet wind tunnel characterization of ultra-high-temperature ceramic matrix composites, Corros. Sci. (2019). doi:10.1016/j.corsci.2018.12.039.
[21] S. Mungiguerra, G.D. Di Martino, A. Cecere, R. Savino, L. Zoli, L. Silvestroni, D. Sciti, Characterization of carbon-fiber reinforced ultra-high-temperature ceramic matrix composites in arc-jet environment, in: Proc. Int. Astronaut. Congr. IAC, Bremen, Germany, 2018.
[22] P. Galizia, S. Failla, L. Zoli, D. Sciti, Tough salami-inspired Cf/ZrB2 UHTCMCs produced by electrophoretic deposition, J. Eur. Ceram. Soc. 38 (2018) 403–409. doi:10.1016/J.JEURCERAMSOC.2017.09.047.
[23] P. Galizia, D. Sciti, F. Saraga, L. Zoli, Off-axis damage tolerance of fiber-reinforced composites for aerospace systems, J. Eur. Ceram. Soc. (2019). doi:10.1016/j.jeurceramsoc.2019.12.038.
[24] C. Sauder, J. Lamon, R. Pailler, The tensile behavior of carbon fibers at high temperatures up to 2400 °C, Carbon N. Y. 42 (2004) 715–725. doi:10.1016/j.carbon.2003.11.020.
[25] P. Galizia, L. Zoli, D. Sciti, Impact of residual stress on thermal damage accumulation, and Young's modulus of fiber-reinforced ultra-high temperature ceramics, Mater. Des. 160 (2018) 803–809. doi:10.1016/J.MATDES.2018.10.019.
[26] J. Sha, S. Wang, J. Dai, Y. Zu, W. Li, R. Sha, High-temperature Mechanical Properties and Their Influence Mechanisms of ZrC-Modified C-SiC Ceramic Matrix Composites up to 1600

°C, Materials (Basel). 13 (2020) 1581. doi:10.3390/ma13071581.
[27] T. Cheng, X. Wang, R. Zhang, Y. Pei, S. Ai, R. He, D. Fang, Y. Yang, Tensile properties of two-dimensional carbon fiber reinforced silicon carbide composites at temperatures up to 2300 °C, J. Eur. Ceram. Soc. 40 (2020) 630–635. doi:10.1016/j.jeurceramsoc.2019.10.030.
[28] Y. Zhang, L. Zhang, L. Cheng, Y. Xu, Tensile behavior and microstructural evolution of a carbon/silicon carbide composite in simulated re-entry environments, Mater. Sci. Eng. A. 473 (2008) 111–118. doi:10.1016/j.msea.2007.05.015.
[29] D. Zhang, P. Hu, S. Dong, Q. Qu, X. Zhang, Effect of pyrolytic carbon coating on the microstructure and fracture behavior of the Cf/ZrB_2-SiC composite, Ceram. Int. 44 (2018) 19612–19618. doi:10.1016/J.CERAMINT.2018.07.210.
[30] J. Marschall, D. Pejakovic, W.G. Fahrenholtz, G.E. Hilmas, F. Panerai, O. Chazot, Temperature Jump Phenomenon During Plasmatron Testing of ZrB_2-SiC Ultrahigh-Temperature Ceramics, J. Thermophys. Heat Transf. 26 (2012) 559–572.